Scheme III. Construction of the DE Ring System (2) of Brevetoxin A (1)[a]

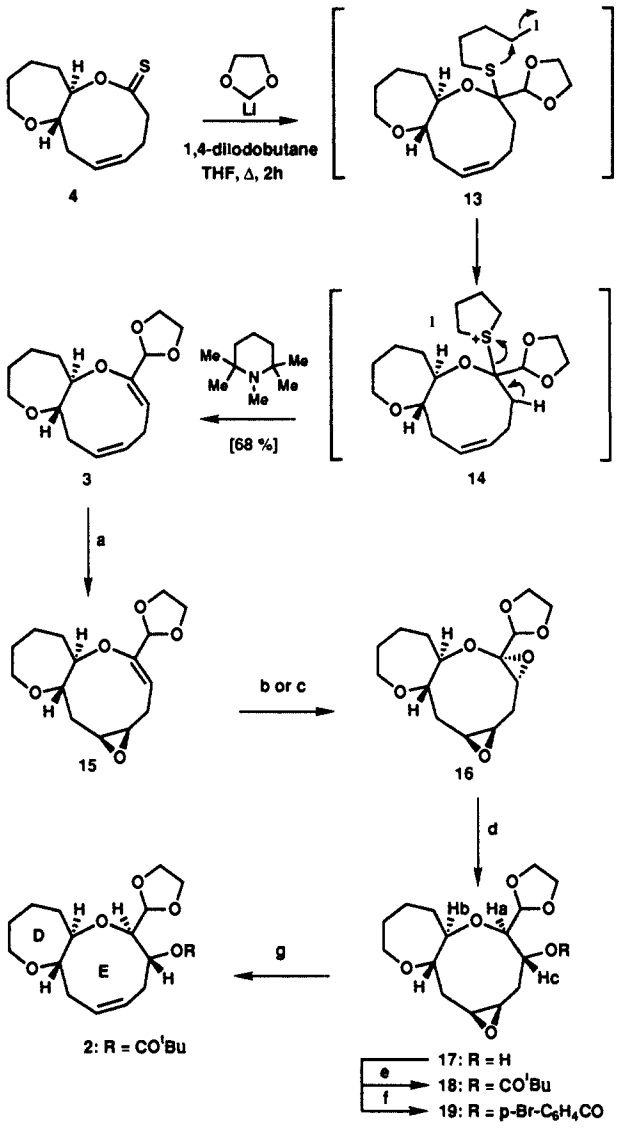

[a] Reagents and conditions: (a) excess dimethyldioxirane, acetone, 0 °C, 20 min, 89%; (b) 5.0 equiv of MMPP, DMF, 25 → 50 °C, 6 h, 75%; (c) 1.5 equiv of mCPBA, 2.0 equiv of $NaHCO_3$, CCl_4, 0 °C, 2 h; (d) excess Et_3SiH, 2.0 equiv of BH_3·THF, 0.1 equiv of TMSOTf, CH_2Cl_2 −20 → 25 °C, 2 h, 56% from **15**; (e) 2.0 equiv of $(CH_3)_3CCOCl$, py, 0 → 25 °C, 18 h, 94%; (f) 2.0 equiv of *p*-BrC_6H_4COCl, py, 0 → 25 °C, 18 h, 90%; (g) 10 equiv of WCl_6, 20 equiv of BuLi, −78 °C, 2 h, 80%.

are out of the plane of the p orbitals of the enol ether (accounting for its lower than expected reactivity toward electrophiles); furthermore, the β-face of the disubstituted double bond appears in this conformation to be more exposed to attack than the α-face, accounting for the predominance of the β-epoxide (Figure 1).[7] Further epoxidation with mCPBA transformed **15** to **16** again with considerable stereocontrol (ca. 4:1 α:β epoxide ratio). Reductive opening of the newly generated epoxide in **16** with Et_3SiH–BH_3·THF–TMSOTf occurred chemo- and regioselectively to furnish the desired skeleton **17** (ca. 56% overall yield from **15**). The stereochemical structure of **17** was tentatively assigned by NMR studies on its pivalate ester **18** (^1H NMR, 500 MHz, $CDCl_3$: NOE between H_a and H_b, ca. 14%; $J_{a,c}$ = 5.6 Hz) and was confirmed by X-ray crystallographic analysis of its *p*-bromobenzoate **19** (see ORTEP drawing, Figure 2). Finally, deoxygenation of **18** with WCl_6–nBuLi[8] led efficiently to the

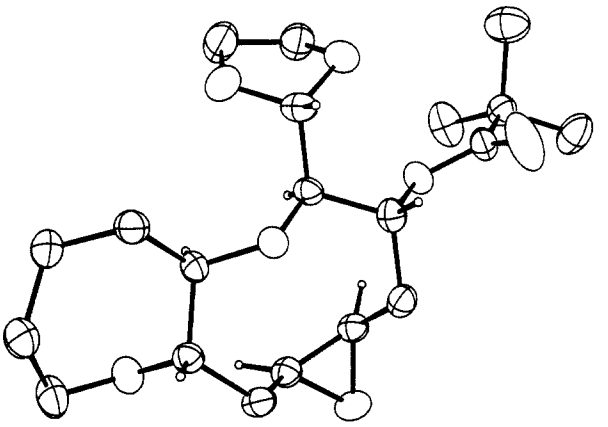

Figure 2. ORTEP drawing of **19**.

targeted intermediate **2** (R = CO'Bu) equipped with the proper functionality for further elaboration.

The described chemistry provides a possible solution to the construction of the challenging oxononacene region of brevetoxin A (**1**). A number of novel reactions and reagents were utilized, and some interesting and unusual conformational effects and reactivity patterns in this ring system were also uncovered. The potential of this technology in the synthesis of **1** and other marine natural products is currently being explored.

Acknowledgment. This work was partly carried out at the University of Pennsylvania. We are grateful to G. T. Furst, J. Dykins, and P. Carroll for their NMR, mass spectral, and X-ray crystallographic assistance, respectively. This work was financially supported by the National Institutes of Health.

Supplementary Material Available: Listing of R_f, $[\alpha]_D$, IR, ^1H NMR, and mass spectral data for compounds **12**, **4**, **3**, **15**, **17**, **18**, and **2** and X-ray crystallographic parameters for **19** (12 pages). Ordering information is given on any current masthead page.

(7) For a discussion of similar facial selectivity in stereoselective reactions of macrocycles, see: Still, W. C.; Galynker, I. *Tetrahedron* **1981**, *37*, 3981.

(8) Sharpless, K. B.; Umbreit, M. A.; Nieh, M. T.; Flood, T. C. *J. Am. Chem. Soc.* **1972**, *94*, 6538.

Deviations from the Simple Two-Parameter Model-Free Approach to the Interpretation of Nitrogen-15 Nuclear Magnetic Relaxation of Proteins

G. Marius Clore,* Attila Szabo, Ad Bax, Lewis E. Kay, Paul C. Driscoll, and Angela M. Gronenborn

Laboratory of Chemical Physics, Building 2
National Institute of Diabetes and Digestive and Kidney Diseases
National Institutes of Health, Bethesda, Maryland 20892

Received January 25, 1990

^{13}C and ^{15}N nuclear magnetic relaxation data provide a wealth of information on the nature of internal motions of macromolecules in solution.[1] In general, the fast internal motions can be described by two model independent quantities:[2] a generalized order parameter **S**, which provides a measure of the amplitude of the motion, and an effective correlation time τ_e. This simple formalism has proved remarkably successful in accounting for relaxation data on small molecules and simple polymers, as well as for fragmentory data obtained from one-dimensional NMR measurements on

(1) London, R. E. In *Magnetic Resonance in Biology*; Cohen, J. S., Ed.; Wiley: New York, 1981; Vol. 1, p 1.
(2) Lipari, G.; Szabo, A. *J. Am. Chem. Soc.* **1982**, *104*, 4546.

Table I. Comparison of Calculated and Observed Nitrogen-15 Relaxation Data for the Backbone Amide Groups of Selected Residues of SNase and IL-1β[a]

	T_1(600), ms	T_2(600), ms	T_1(500), ms	T_2(500), ms	T_1(270), ms	NOE-(600)	NOE-(500)	S^2	τ_e, ns	S_f^2	S_s^2	τ_s, ns
							SNase Leu-7					
obsd	740 ± 6		618 ± 24	136 ± 5	378 ± 54		0.46 ± 0.1					
calcd, eq 1	740	129	620	135	315	-0.43	-0.47	0.54 ± 0.004	0.37 ± 0.007			
calcd, eq 4	738	130	627	137	320	0.56	0.48			0.53 ± 0.006	0.78 ± 0.007	0.68 ± 0.006	1.5 ± 0.08
							SNase Ile-18					
obsd	785 ± 15		635 ± 10	123 ± 3	339 ± 80		0.64 ± 0.1					
calcd, eq 1	784	117	644	123	310	-0.26	-0.20	0.62 ± 0.01	0.24 ± 0.01			
calcd, eq 4	781	116	643	123	307	0.69	0.64			0.61 ± 0.006	0.77 ± 0.006	0.80 ± 0.006	1.8 ± 0.18
							IL-1β Gly-22					
obsd	784 ± 7	210 ± 11				0.32 ± 0.01						
calcd, eq 1	784	210	684	216	403	-1.14	-1.21	0.33 ± 0.014	0.31 ± 0.008			
calcd, eq 4	782	210	696	219	404	0.33	0.17			0.31 ± 0.005	0.68 ± 0.006	0.46 ± 0.007	1.2 ± 0.04
							IL-1β Asp-35					
obsd	739 ± 6	128 ± 2				0.68 ± 0.1						
calcd, eq 1	739	128	607	134	300	-0.24	-0.18	0.61 ± 0.004	0.25 ± 0.007			
calcd, eq 4	736	128	611	133	299	0.70	0.65			0.59 ± 0.004	0.76 ± 0.008	0.78 ± 0.005	2.0 ± 0.3

[a] The T_1, T_2, and NOE data were recorded by two-dimensional ^{15}N inverse detected heteronuclear NMR spectroscopy using the pulse schemes described in ref 7. The rotational correlation times for SNase and IL-1β are 9.1 ± 0.05 and 8.3 ± 0.05 ns, respectively,[7,9] and were obtained from a global fit of the T_1/T_2 ratios of all residues, excluding those with either a ^{15}N–^{1}H NOE below 0.6 or unusually long T_2 values due to chemical exchange, as described in ref 7. In the case of SNase, data were recorded at spectrometer frequencies of 600, 500, and 270 MHz, while in the case of IL-1β, data were recorded only at 600 MHz. Both proteins were uniformly labeled (>95%) with ^{15}N. The errors in the T_1 and T_2 data are the standard deviations obtained from a least-squares fit of a single exponential decay to the time dependence of the relaxation data measured at six time points. Best fitting to all the relaxation data simultaneously was carried out by using Powell's method of nonlinear optimization.[14] Note that the NOE data was excluded in the best fits using eq 1, as inclusion of the NOE data in this case results in none of the relaxation data being satisfied. In the case of fits using eq 1, S^2 and τ_e were varied, while for fits using eq 4, S^2, S_f^2, and τ_s were varied. S_s^2 is calculated from S^2 and S_f^2 by using eq 3.

peptides and proteins.[3-6] With the development of sensitive ^{1}H-detected two-dimensional heteronuclear NMR experiments for the measurement of heteronuclear relaxation data,[7,8] the methodology is now at hand to obtain a comprehensive picture of internal motions in proteins. While studying the backbone dynamics of two recombinant proteins, staphylococcal nuclease[7] (SNase, 149 residues) and interleukin-1β[9] (IL-1β, 153 residues), in this manner, we have noticed that the ^{15}N T_1, T_2, and NOE data for the backbone amide groups of certain residues cannot be accounted for by the simple two-parameter model-free approach and necessitate the introduction of two distinct correlation times to describe the internal motions.

In the model-free formalism of Lipari and Szabo,[2] the spectral density function for a molecule undergoing isotropic tumbling is given by

$$J(\omega) = \mathbf{S}^2\tau_R/(1 + \omega^2\tau_R^2) + (1 - \mathbf{S}^2)\tau/(1 + \omega^2\tau^2) \quad (1)$$

which corresponds to an internal correlation function of $C_l(t) = \mathbf{S}^2 + (1 - \mathbf{S}^2)e^{-t/\tau_e}$, where $\mathbf{S}$ is the generalized order parameter, τ_R is the overall isotropic rotational correlation time of the molecule, and $\tau = \tau_R\tau_e/(\tau_R + \tau_e)$ where τ_e is a single effective correlation time describing the internal motions. The T_1 and T_2 relaxation times and the NOE enhancement of an amide ^{15}N spin relaxed by dipolar coupling to a directly bonded proton and by chemical shift anisotropy are related to the spectral density function by the well-known[10] expressions given in ref 7.

Excluding residues where T_2 exchange line broadening is present (four in SNase and 42 in IL-1β), we have found that, for all but four residues of SNase and 32 residues of IL-1β, the available ^{15}N relaxation data can be accounted for within the errors of the experimental data (at both 500 and 600 MHz, <5% for T_1 and T_2, and in the majority of cases <2% for T_1; ±0.1 for the NOE) by using the simplified spectral density function $J(\omega) = \mathbf{S}^2\tau_R/(1 + \omega^2\tau_R)$ with a single value of τ_R (9.1 and 8.3 ns for SNase and IL-1β, respectively) and $\mathbf{S}^2$ in the range $0.7 \le \mathbf{S}^2 \le 0.95$, indicating that τ_e is smaller than about 50 ps and that the two proteins reorient isotropically in solution. For the exceptional residues, we find that while eq 1 can account for the ^{15}N T_1 and T_2 data at several spectrometer frequencies, it fails to account for the ^{1}H–^{15}N NOE data. In particular, on the basis of the best fit to the T_1 and T_2 data using eq 1, the calculated values for the NOE are either too small or negative, whereas the observed ones are positive. This point is illustrated in Table I for Leu-7 and Ile-18 of SNase and Gly-22 and Asp-35 of IL-1β. On the basis of the best fit to the T_1 and NOE data (not shown), the calculated values for T_2 are 20–100% too small for these residues.

The discrepancy indicates that the time evolution of the internal reorientational correlation function that is probed by NMR must be highly nonexponential with slow components that are not in the extreme narrowing limit. The simplest functional form for the internal correlation function that can describe such behavior is $C_l(t) = \mathbf{S}^2 + A_fe^{-t/\tau_f} + A_se^{-t/\tau_s}$ with $\mathbf{S}^2 + A_f + A_s = 1$. When the fast ($\tau_f$) and slow ($\tau_s$) correlation times differ by at least 1 order of magnitude, $C_l(t)$ reaches an intermediate plateau value of $1 - A_f$, before finally leveling off at $\mathbf{S}^2$. Thus, when such a separation of time scales exists, one can interpret $1 - A_f$ as the generalized order parameter for fast motions, $\mathbf{S}_f^2$. Hence, one has $C_l(t) = \mathbf{S}^2 + (1 - \mathbf{S}_f^2)e^{-t/\tau_f} + (\mathbf{S}_f^2 - \mathbf{S}^2)e^{-t/\tau_s}$ so that the spectral density in the case of isotropic overall reorientation is

$$J(\omega) = \frac{\mathbf{S}^2\tau_R}{1 + (\omega\tau_R)^2} + \frac{(1 - \mathbf{S}_f^2)\tau_f'}{1 + (\omega\tau_f')^2} + \frac{(\mathbf{S}_f^2 - \mathbf{S}^2)\tau_s'}{1 + (\omega\tau_s')^2} \quad (2)$$

(3) Lipari, G.; Szabo, A. *J. Am. Chem. Soc.* **1982**, *104*, 4559.
(4) McCain, D. C.; Markley, J. L. *J. Am. Chem. Soc.* **1986**, *108*, 4259.
(5) Weaver, A. J.; Kemple, M. D.; Predergast, F. G. *Biphys. J.* **1988**, *54*, 1.
(6) Dellwo, M. J.; Wand, A. J. *J. Am. Chem. Soc.* **1989**, *111*, 4571.
(7) Kay, L. E.; Torchia, D. A.; Bax, A. *Biochemistry* **1989**, *28*, 8972.
(8) Nirmala, N. R.; Wagner, G. *J. Magn. Reson.* **1989**, *82*, 659.
(9) Clore, G. M.; Driscoll, P. C.; Wingfield, P. T.; Gronenborn, A. M. *Biochemistry* In press.
(10) Abragham, A. *The Principles of Nuclear Magnetism*; Clarendon Press: Oxford, 1961.

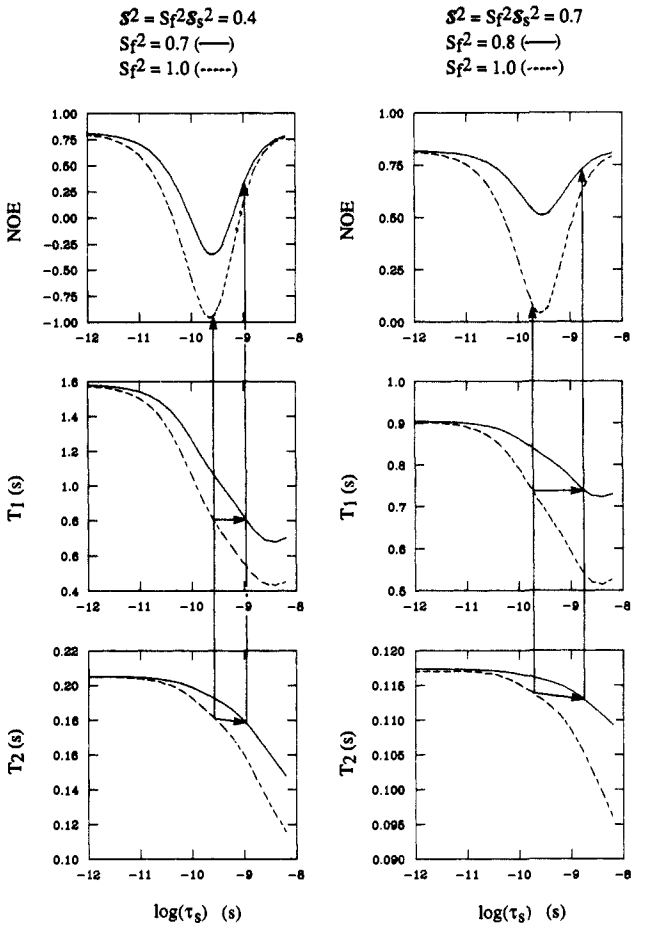

Figure 1. Dependence of the NOE, T_1, and T_2 ^{15}N relaxation parameters on the effective correlation time (τ_s) for internal motions for a spectral density function with a single internal motion ($S_f^2 = 1$; dashed lines) and two internal motions ($S_f^2 < 1$; solid lines). The curves are calculated by using the spectral density function given by eq 4, a rotational correlation time of 8.3 ns, a ^{15}N frequency of 60.8 MHz, and a ^1H frequency of 600 MHz. When $S_f^2 = 1$, the spectral density function (eq 4) reduces to the single internal motion spectral density function (eq 1) of the Lipari and Szabo treatment.[2]

with $\tau_i' = \tau_i\tau_R/(\tau_R + \tau_i)$, i = f, s. Note that eq 2 reduces to eq 1 when $S_f^2 = 1$ or $S^2 = S_f^2$. If it is assumed that the fast internal motions are axially symmetric (in which case $S_f^2 = S_f^2$ where S_f is the usual order parameter) and independent of the slow motions, then one can decompose the total generalized order parameter as

$$S^2 = S_f^2 S_s^2 \tag{3}$$

where S_s is the generalized order parameter describing the slow motions.

To find the simplest description consistent with the available data, we assume that τ_f is sufficiently small so as to make a negligible contribution to the relaxation parameters and hence use the spectral density

$$J(\omega) = \frac{S^2\tau_R}{1 + (\omega\tau_R)^2} + \frac{(S_f^2 - S^2)\tau_s'}{1 + (\omega\tau_s')^2} \tag{4}$$

to fit the data. The best-fit values of S^2, S_f^2, and τ_s together with the calculated T_1, T_2, and NOE values are given in Table I. It will be noted that the generalized order parameters extracted by using eq 1 and eq 4 are essentially the same.

The values of the generalized order parameters for slow motions can be obtained by using eq 3 and interpreted within the framework of some model to get a physical picture of the amplitude of the motions. For example, if the fast motions occur in a cone of semiangle θ_0, $S_f = (\cos\theta_0)(1 + \cos\theta_0)/2$, and, if the slow motions are described by a two site jump model, $S_s^2 = (1 + 3\cos^2\varphi)/4$ where φ is the angle between the two orientations of the N-H bond.

The effect of using spectral density function eq 4 compared to eq 1 is easily understood by noting that the calculated values of τ_e (0.2-0.3 ns) are 1 order of magnitude smaller than those of τ_s (1-3) ns. For $\tau_R \sim 8$ ns and $\omega_N = 2\pi \times 60.8$ MHz, the NOE reaches a minimum value at an internal correlation time of ~0.25 ns. Thus the shift in internal correlation time to larger values which occurs in the two internal correlation time formulation results in larger values of the NOE, while the values of T_1 and T_2 are unaffected. This is illustrated in Figure 1.

These results clearly indicate that the ^{15}N relaxation data reflect the existence of internal motions of significant amplitude both on the very fast (extreme narrowing) and on the relatively slow time scales in certain regions of these proteins. Hence the correlation function for the internal motions of these residues can no longer be approximated to a single exponential of the Lipari and Szabo treatment,[2] but rather requires at least two exponentials. The slow correlation time, of the order of 1-3 ns, is somewhat faster than the overall rotational correlation time (8-9 ns) and can have a significant amplitude. The very fast motions may reflect the fast random thermal motions that are manifested in molecular dynamics calculations.[11-13]

Acknowledgment. This work was supported by the AIDS Directed Anti-Viral Program of the Office of the Director of the National Institutes of Health (G.M.C., A.M.G., A.B.).

(11) Karplus, M.; McCammon, J. A. *Crit. Rev. Biochem.* **1981**, *9*, 293.
(12) Lippari, G.; Szabo, A.; Levy, R. M. *Nature* **1982**, *300*, 197.
(13) Levy, R. M.; Karplus, M.; McCammon, J. A. *J. Am. Chem. Soc.* **1981**, *103*, 994.
(14) Powell, M. J. D. *Comput. J.* **1965**, *7*, 303.

Total Synthesis of (+)-Latrunculin A

James D. White* and Motoji Kawasaki

Department of Chemistry, Oregon State University
Corvallis, Oregon 97331-4003

Received March 5, 1990

The ichthyotoxin latrunculin A (**1**), originally isolated from the Red Sea sponge *Latrunculia magnifica* (Keller),[1] has also been found in the Pacific nudibranch *Chromodoris elisabethina*[2] and in the Fijian sponge *Spongia mycofijiensis*.[3] Its biological properties, particularly its powerful effect on the cytoskeletal protein actin[4] and its ability to reversibly disrupt microfilament organization,[5] have been compared to those of cytochalasin D.[6] Synthesis of the structurally related, companion metabolite latrunculin B (**2**) was reported in 1986 by Smith et al.;[7] we now describe the synthesis of **1** by a pathway that is significantly different from the published route to **2**.[8]

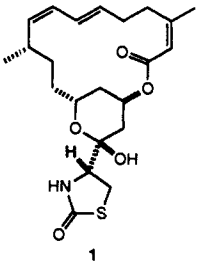

1

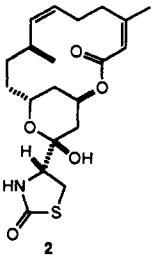

2

(1) (a) Groweiss, A.; Shmueli, U.; Kashman, Y. *J. Org. Chem.* **1983**, *48*, 3512 and references cited. (b) Kashman, Y.; Groweiss, A.; Lidor, R.; Blasberger, D.; Carmely, S. *Tetrahedron* **1985**, *41*, 1905.
(2) Okuda, R. K.; Scheuer, P. J. *Experientia* **1985**, *41*, 1355.

0002-7863/90/1512-4991$02.50/0